Shear Resonance Frequencies of Alluvial Valleys by Rayleigh's Method

Roberto Paolucci

A simple approach based on Rayleigh's method has been used for the fast estimation of the shear resonance frequencies of alluvial valleys. After an example considering a 1-D non-homogeneous configuration, the method is applied to 2-D and 3-D homogeneous simple-shaped valleys, for which numerical solutions exist in the literature. The application of the proposed method to deep non-homogeneous sedimentary basins is then illustrated, showing that even in a rather complex soil configuration the prediction errors do not exceed about 20%. If one considers the uncertainties related to the determination of the mechanical properties of a real soil configuration, this prediction is quite reasonable. Furthermore, the predicted fundamental frequency always provides an upper limit of the true value. Although the predicted results are not very accurate, the proposed procedure may be helpful in several practical applications, such as in the case of complex geological configurations, where the problem exists of assessing in which frequency band 1-D resonance will differ significantly from the 2-D or 3-D one. This is important to decide whether performing more sophisticated analyses of site effects and whether the use of standard code spectral shapes is appropriate.

INTRODUCTION

Sedimentary basins and local stratigraphic irregularities have long been recognized to affect earthquake ground motion selectively, with large amplifications at the resonance frequencies of the geological structure (e.g., Aki, 1993). While the 1-D case of horizontally layered soil profiles is routinely dealt with in engineering practice using linear and non-linear methods (e.g., Schnabel et al., 1972), the computational requirements for the seismic response analysis of 2-D/3-D structures are still heavy.

In fact, the computer effort to run 2-D models of real geological configurations may range from few hours to several days, depending on the problem and on the available software and machines, while the seismic analysis of 3-D models is still confined to few research applications (e.g., Frankel and Vidale, 1992; Olsen et al., 1995; Paolucci et al., 1999; Graves, 1998). The demand on human resources is also non negligible, since the construction of complex 3-D models may require up to several weeks also for well trained experts of mesh generation.

Methods for fast computation of seismic wave propagation in 2-D/3-D structures are few, and mainly limited to homogeneous simple-shaped configurations (Paolucci et al., 1992; Rodríguez-Zúñiga et al., 1995), so that their application to real cases may be questionable.

Dept. of Structural Engineering, Politecnico di Milano, Piazza L. da Vinci 32, I-20133 Milano, Italy

©*Earthquake Spectra*, Volume 15, No. 3, August 1999

Therefore, although research on seismic site effects has made much progress in the last 15 years, especially after the 1985 Michoacán earthquake that caused enormous destruction in Mexico City, 2-D/3-D site effects are seldom accounted for in the engineering practice. Besides, in up-to-date seismic codes such as Uniform Building Code (1997), the indications on how 2-D/3-D effects can be practically quantified are absent, while only recently Chávez-García and Faccioli (1999) have suggested a procedure to modify design spectra to account for amplification on 2-D alluvial valleys.

In this paper, a simple method is illustrated for estimating the shear resonance frequencies of 2-D/3-D non-homogeneous sediment-filled valleys. The estimation is based on Rayleigh's method, an energy approach widely used in structural dynamics for the fast evaluation of the resonance frequencies of multi-degrees-of-freedom systems (e.g., Meirovitch, 1967; Clough and Penzien, 1975).

A procedure based on such approach was already devised by Dobry et al. (1976) for estimating the fundamental period of 1-D soil profiles, with errors up to about 10 per cent. In this paper it will be shown that also the extension to 2-D/3-D sedimentary valleys gives satisfactory results, with prediction errors that are negligible for homogeneous configurations and grow up to about 20% for valleys with sharp discontinuities of soil properties.

METHOD

The basic idea underlying Rayleigh's method is that the motion of an undamped elastic system in one of its natural modes can be approximated by that of a single-degree-of-freedom system. For simplicity, I will refer in this section to the fundamental (1st) mode defined by the circular frequency $\omega_0 = 2\pi f_0$. If V denotes the elastic strain energy of the system, and T its kinetic energy, conservation of the total energy of the elastic system ensures that

$$V_{max}=T_{max} \tag{1}$$

where V_{max} and T_{max} are the maximum values of V and T.

In the general case of a 3-D vibrating bounded medium, defined in the domain Ω, the displacement $s_k(\underline{x},t)$ corresponding to harmonic vibrations with circular frequency ω_0 can be expressed as:

$$s_k(\underline{x},t) = \psi_k(\underline{x})e^{i\omega_0 t}, \tag{2}$$

where $\underline{x}$ denotes position in the 3-D space, i = imaginary unit, t = time, and $\psi_k(\underline{x})$ the mode-shape along the k-th direction. The kinetic energy T of the system can be calculated as:

$$T(t) = \int_{\Omega}\frac{1}{2}\rho(\underline{x})\left(\frac{\partial s_k}{\partial t}\right)^2 d\Omega = -\omega_0{}^2 e^{2i\omega_0 t}\int_{\Omega}\frac{1}{2}\rho(\underline{x})\psi_k{}^2(\underline{x})d\Omega, \tag{3}$$

hence:

$$T_{max} = \max_t T(t) = -\omega_0{}^2\int_{\Omega}\frac{1}{2}\rho(\underline{x})\psi_k{}^2(\underline{x})d\Omega. \tag{4}$$

The strain energy V is defined as:

$$V(t) = \int_{\Omega} \frac{1}{2} \sigma_{jl}(\underline{x}) \varepsilon_{jl}(\underline{x}) d\Omega \tag{5}$$

where $\varepsilon_{jl} = s_{j,l} + s_{l,j}$ is the strain tensor and $\sigma_{jl} = \lambda \varepsilon_{ii} \delta_{jl} + 2\mu \varepsilon_{jl}$ is the stress tensor calculated by Hooke's law. δ_{jl} is Kronecker's symbol, λ and μ are Lamé's constants. As for T_{max}, the maximum value V_{max} is obtained when $\left| e^{2i\omega_0 t} \right| = 1$. Note that in Equation 5 only terms involving the k-th component of motion shall be retained. Equating the absolute values of T_{max} and V_{max}, one obtains:

$$\omega_0^2 = \frac{\int_{\Omega} \sigma_{jl}(\underline{x}) \varepsilon_{jl}(\underline{x}) d\Omega}{\int_{\Omega} \rho(\underline{x}) \psi_k^2(\underline{x}) d\Omega} \tag{6}$$

Equation 6 provides the exact value of the fundamental frequency of the system if the true mode-shape $\psi_k(\underline{x})$ is selected. However, since the exact solution is seldom available, the value of ω_0 can be closely approached using a suitable approximation of $\psi_k(\underline{x})$.

The approximated mode-shapes must satisfy both geometric and stress compatibility at boundaries. However, as demonstrated by Meirovitch (1967), the second requirement can be relaxed and such approximated mode-shapes can be chosen in the larger set of admissible functions that satisfy only the geometric compatibility. As will be shown later, this assumption simplifies significantly the choice of the set of admissible mode-shapes for 2-D/3-D alluvial valleys.

A further important property of Rayleigh's method is that the chosen admissible mode-shape will provide an upper bound to the true fundamental frequency. Indeed, as shown by Clough and Penzien (1975), any admissible shape other than the true one requires additional constraints for equilibrium to be satisfied. Such constraints cause the stiffening of the system and, consequently, an increase of the computed frequency. Therefore, if we denote by $\hat{\psi}_k(\underline{x})$ a set of admissible shape functions and by $\hat{\sigma}_{jl}$ and $\hat{\varepsilon}_{jl}$ the corresponding stress and strain tensors, the true fundamental frequency can be approached as follows:

$$\omega_0^2 \leq \min_{\hat{\psi}_k} \frac{\int_{\Omega} \hat{\sigma}_{jl}(\underline{x}) \hat{\varepsilon}_{jl}(\underline{x}) d\Omega}{\int_{\Omega} \rho(\underline{x}) \hat{\psi}_k^2(\underline{x}) d\Omega} \tag{7}$$

It is worth noting that this procedure is similar to the upper bound approach of the yield design theory, for bearing capacity calculations (e.g., Chen and Liu, 1990; Paolucci and Pecker, 1997). In the latter case the limit load is computed by finding, in a set of admissible rupture mechanisms, the mechanism that minimizes the ratio between the maximum power of resisting forces and the power of external forces.

EXAMPLE OF APPLICATION TO A 1-D SOIL PROFILE

To illustrate by a simple example the application of Rayleigh's method to geological structures, consider a homogeneous layer of depth H, soil density ρ and shear modulus μ,

overlying a rigid bedrock (Figure 1). In this case, the exact expression of the fundamental mode in the horizontal direction (e.g., x_1) is:

$$\psi_1(x_3) = A\cos\left(\frac{\pi x_3}{2H}\right) \tag{8}$$

where x_3 is the vertical axis and A is a multiplication factor that will be omitted hereafter, since it does not affect the calculation of resonance frequencies. Therefore, the displacement field is $\underline{s} = \left[\psi_1(x_3)e^{i\omega t} \quad 0 \quad 0\right]$, and $\varepsilon_{13} = \varepsilon_{31} = \frac{1}{2}\frac{\partial s_1}{\partial x_3}$ are the only non-vanishing components of the strain tensor. Recalling Hooke's law, Equation 6 reduces to

$$\omega_0{}^2 = \frac{\int_0^H \mu\left(\frac{\partial \psi_1}{\partial x_3}\right)^2 dx_3}{\int_0^H \rho\psi_1{}^2(x_3)dx_3} \tag{9}$$

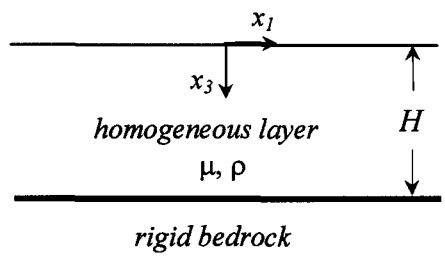

Figure 1. Homogeneous layer over rigid bedrock.

Introducing Equation 8 in Equation 9 and denoting by $\beta = \sqrt{\mu/\rho}$ the propagation velocity of shear waves, it is easy to find that the fundamental resonance frequency of the layer is $f_0 = \beta/4H$, that coincides with the well known theoretical value. Rayleigh's method provides in this case the exact solution because the selected mode-shape (Equation 8) is the true one. Any other mode-shape satisfying the boundary conditions

$$s_1\big|_{x_3=H} = 0, \quad \partial s_1/\partial x_3\big|_{x_3=0} = 0 \tag{10}$$

will provide an estimated f_0 not smaller than the true one.

Consider now a non-homogeneous soil layer over rigid base, with constant density and shear wave velocity $\beta(x_3)$ variable with depth. For the particular choice:

$$\beta(x_3) = \beta_0\left(1 + 3\alpha\frac{x_3}{H}\right)^{2/3}, \tag{11}$$

where

$$\alpha = \frac{1}{3}\left[\left(\frac{\beta_H}{\beta_0}\right)^{3/2} - 1\right], \quad \beta_0 = \beta(x_3{=}0), \quad \beta_H = \beta(x_3{=}H), \tag{12}$$

a closed form theoretical solution of the 1-D shear wave propagation equation can be derived (Schreyer, 1977), whence the fundamental frequency f_0 of the layer is obtained as the smallest root of the following eigenvalues equation:

$$\frac{\omega_0 H}{\alpha\beta_0} + \tan\left[\frac{\omega_0 H}{\alpha\beta_0}\left(\sqrt{\frac{\beta_H}{\beta_0} - 1}\right)\right] = 0. \tag{13}$$

The proposed procedure based on Rayleigh's method is used to approach the theoretical value given by Equation 13. Introducing the following set of admissible mode-shapes:

$$\hat{\psi}_1(x_3) = \cos^r\left(\frac{\pi x_3}{2H}\right) \quad (r \geq 1), \tag{14}$$

inequality (Equation 7) reduces to:

$$\omega_0^2 \leq \min_r \frac{\int_0^H \mu(x_3)\left(\frac{\partial \hat{\psi}_1}{\partial x_3}\right)^2 dx_3}{\int_0^H \rho \hat{\psi}_1^2(x_3) dx_3}. \tag{15}$$

The integrals in Equation 15 are calculated numerically with Gauss quadrature formulas and a standard minimization procedure with respect to r is used. The theoretical f_0 values, obtained by Equation 13 as a function of $\beta_0/4H$ and for different values of the ratio β_H/β_0, are compared in Figure 2 with those provided by the present method. With increasing values of β_H/β_0, the agreement gets worse but the maximum error with respect to the theoretical values does not exceed 4%.

The theoretical mode-shape is compared in Figure 3 with Equation 14 setting r=1 and r=1.43. The latter value minimizes Equation 14 in the case $\beta_0/4H$=1 s^{-1} and β_H/β_0 = 3. In this case, Rayleigh's predictions are very good in terms of f_0, with an error lower than 1% (see Figure 2), but the mode-shape does not correctly reproduce the true one. This is a typical feature of Rayleigh's method, for which the errors arising in the estimation of the resonance frequency are much smaller than those in the mode-shape (Prentis, 1970).

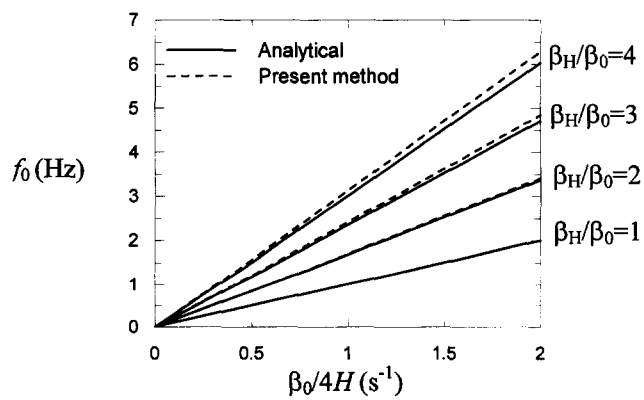

Figure 2. Fundamental SH frequencies of a heterogeneous soil profile with shear wave velocity defined by Equation 11.

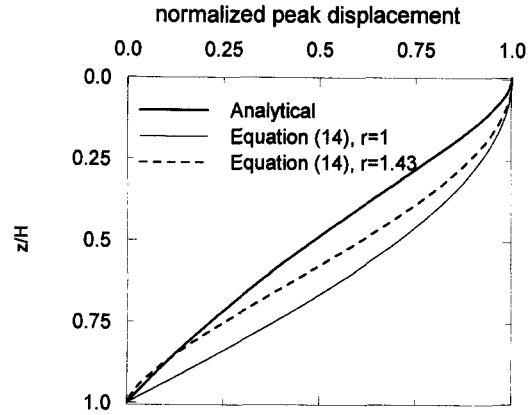

Figure 3. Fundamental mode-shape of soil profile (11) with $\beta_0/4H=1$ (s^{-1}) and $\beta_H/\beta_0=3$, compared with the results of the present method.

APPLICATION TO 2-D HOMOGENEOUS VALLEYS

The two-dimensional resonance of homogeneous symmetric sediment valleys was analysed by Bard and Bouchon (1985), who performed a detailed parametric study using the Aki-Larner method for numerical wave propagation. The main patterns of shear natural modes of 2-D valleys were identified in that study. Namely, it was recognized that the first natural mode shows itself as an in-phase motion across the whole valley, that decreases regularly from the center of the valley to the edges. The first higher mode is antisymmetric and is characterized by a displacement node at the valley center and maxima at mid-edges. Being antisymmetric, it appears in the case of oblique incidence, or of non-symmetric valleys. Higher modes are further described in the quoted paper. The observed patterns are qualitatively similar for both out-of-plane and in-plane motions.

ANTI-PLANE (SH) CASE

To illustrate by a simple application the capabilities of the proposed method for 2-D geological configurations, the case of flat homogeneous valleys, overlying a rigid bedrock, is first considered (Figure 4).

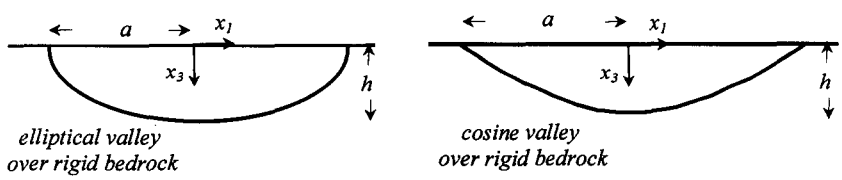

Figure 4. Elliptical and cosine-shaped valleys over rigid bedrock.

Let the interface Γ between the valley and the bedrock be described by the following equations:

$$f(x_1,x_3) = 1 - \frac{x_1^2}{a^2} - \frac{x_3^2}{h^2} \qquad \text{(elliptical valley)} \qquad (16a)$$

$$f(x_1,x_3) = \cos\left(\frac{\pi x_1}{2a}\right) - \frac{x_3}{h} \qquad \text{(cosine valley)} \qquad (16b)$$

It was shown elsewhere (Bard and Bouchon, 1985; Jiang and Kuribayashi, 1988) that the assumption of a rigid bedrock has a negligible influence on the resonance frequencies of vibration of the valley, while it does affect the amplification values. However, as noted before, the present method only aims at predicting the resonance frequencies, while nothing can be said about amplifications.

Among the possible mode-shapes for SH vibrations, we choose the following:

$$\hat{\psi}_2(x_1,x_3) = \cos^r\left(\frac{\pi}{2}(1-f(x_1,x_3))\right)\sin^{(2s+1)}\left(\frac{(n+1)\pi}{2}(1+x_1/a)\right)\cos^t\left(\frac{(2m+1)\pi}{2}\frac{x_3}{h}\right) \qquad (17)$$

where $f(x_1,x_3)$ is either Equation 16a or 16b. Equation 17 is a generalization of the exact expression of the displacement field for a rectangular inclusion in a halfspace reported by Bard and Bouchon (1985), and complies with the qualitative features of the vibration modes mentioned previously. In Equation 17, $r \geq 1$ and $t \geq 1$ are real parameters, $s = 0,1,..$ is an integer parameter, while the integer parameters m and n define the mode number in the vertical and horizontal directions, respectively. A picture of Equation 17 for the cosine valley is illustrated in Figure 5a for the case r=1, t=1, s=0, m=0, n=0 (first natural mode) and in Figure 5b for the case r=1, t=1, s=0, m=0, n=1 (second natural mode).

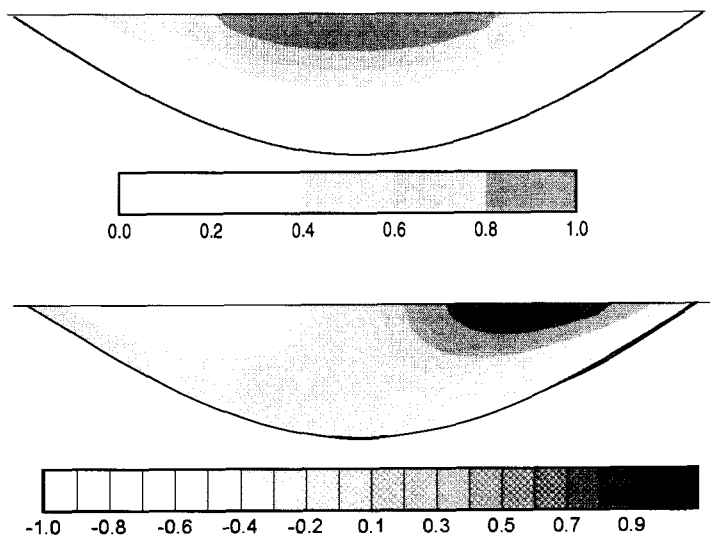

Figure 5. Gray-scale plot of Equation 17, for the approximation of *(top)* the first (n=0) and *(bottom)* the second (n=1) natural modes of a cosine-shaped valley. The other parameters of (17) are set to r=1, s=0, t=1, m=0.

Using Equation 17 as an approximation of the true mode-shape, the expressions (Equations 4 and 5) of the kinetic and strain energy are derived. Subsequently, Equation 7 is applied and the resonance frequencies corresponding to different combinations of m and n can be found by a standard minimization procedure with respect to parameters r, s, t. In agreement with Bard and Bouchon (1985), the first few natural modes (up to the third) are generally obtained setting m=0, so that this parameter will be omitted hereafter. Also, the minimum is generally found for s=0, while t and r are slightly larger than 1.

The results obtained for the first natural mode (n=0) are depicted in Figure 6 (SH case) and compared with the empirical formula proposed by Bard and Bouchon (1985). Note that the depth of the valley (h) is divided by a, where $2a$ is the equivalent width of the valley, i.e., the length over which the local sediment thickness is greater than $h/2$. The frequency values in the vertical axis of Figure 6 are divided by f_h, where $f_h=\beta/4h$ is the fundamental shear resonance frequency of a 1-D homogeneous layer of depth h. A satisfactory agreement is found, showing that the selected mode-shape (Equation 17) is a good approximation of the true one.

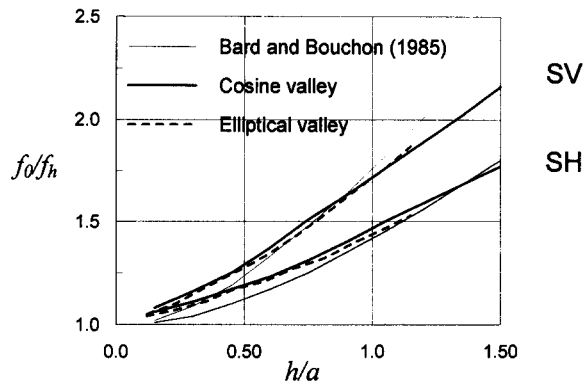

Figure 6. Comparison of the fundamental resonance frequencies of alluvial valleys calculated according to the empirical formula of Bard and Bouchon (1985) with the results of the present method. The equivalent valley half-width (a) and the normalization frequency ($f_h=\beta/4h$) are defined in the text.

It is important to note that the boundary conditions

$$\hat{\psi}_2|_\Gamma = 0 \tag{18a}$$

$$\partial\hat{\psi}_2 / \partial x_3|_{x_3=0} = 0 \tag{18b}$$

are matched in the case of elliptical valley (Equation 16a), since $\partial f / \partial x_3|_{x_3=0} = 0$, while the approximation (Equation 16b) for the cosine valley does not match condition (Equation 18b). However, as noted previously, Rayleigh's method can still be applied with shape functions that satisfy only the geometric boundary conditions, of the type (Equation 18a). Indeed, the consistency of the results obtained for the two valleys indicates that violation of Equation 18b has no practical influence, and Equation 16b may be considered as a satisfactory approximation also for the cosine valley.

Other mode-shapes have been selected as alternatives to Equation 17, but the latter was found to give in most cases the best upper-bound approximation.

IN-PLANE (SV) CASE

In analogy with Equation 17, a displacement field $\hat{\underline{s}} = \left[\hat{\psi}_1(x_1,x_3)e^{i\omega t} \quad 0 \quad \hat{\psi}_3(x_1,x_3)e^{i\omega t}\right]$ is chosen, defined by the following mode-shapes:

$$\hat{\psi}_1(x_1,x_3) = \cos^r\left(\frac{\pi}{2}(1-f(x_1,x_3))\right)\sin^{(2s+1)}\left(\frac{(n+1)\pi}{2}(1+x_1/a)\right)\cos^t\left(\frac{(2m+1)\pi}{2}\frac{x_3}{h}\right) \quad (19a)$$

$$\hat{\psi}_3(x_1,x_3) = 0 \quad (19b)$$

The boundary conditions are now the following:

$$\hat{\psi}_1\big|_\Gamma = \hat{\psi}_3\big|_\Gamma = 0 \quad (20a)$$

$$(\lambda+2\mu)\frac{\partial\hat{\psi}_3}{\partial x_3}\bigg|_{x_3=0} + \lambda\frac{\partial\hat{\psi}_1}{\partial x_1}\bigg|_{x_3=0} = 0 \quad (20b)$$

$$\mu\left(\frac{\partial\hat{\psi}_3}{\partial x_1} + \frac{\partial\hat{\psi}_1}{\partial x_3}\right)\bigg|_{x_3=0} = 0, \quad (20c)$$

that define the rigid valley bottom (Equation 20a) and the stress-free surface condition (Equations 20b and 20c). It is easy to verify that the mode-shapes (Equation 19) satisfy only the geometric conditions (Equation 20a) while the natural boundary conditions (Equations 20b and 20c) are not generally satisfied.

The adequacy of the selected shapes (Equation 19) for the SV case is demonstrated in Figure 6. Again, there is a reasonable agreement between the elliptical and cosine-shaped valley with the approximate formula of Bard and Bouchon (1985).

The first shear resonance frequencies (up to the third mode) obtained by the present approach are shown in Figure 7 for the case of elliptical homogeneous valleys as a function of *h/a*. For a given *h/a*, the ratio between the resonance frequency of the *n*th natural mode with respect to the *(n+1)*th is about 70%. This may be a practical rule of thumb for estimating higher vibration frequencies, based on the fundamental one.

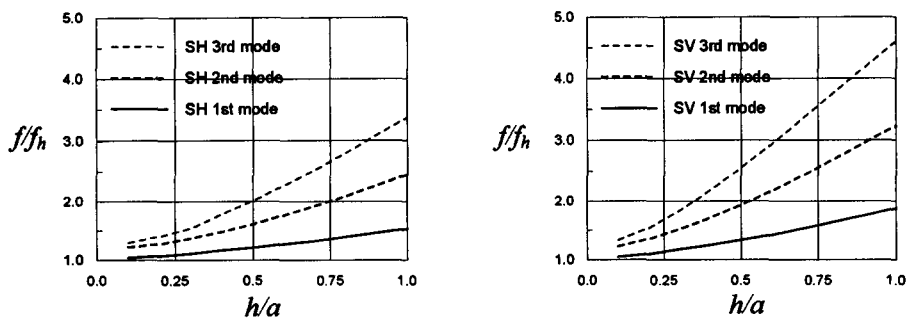

Figure 7. Resonance frequencies corresponding to the first three natural modes of an elliptical valley, calculated by the present method. Left: SH case. Right: SV case.

APPLICATION TO 3-D HOMOGENEOUS ALLUVIAL VALLEYS

To study the capability of the present method for 3-D geological structures, a cylindrical homogeneous inclusion embedded in half-space is considered (Figure 8). The inclusion has radius R=400 m and depth h=100 m. The density is ρ=2500 kg/m^3 throughout the model, while shear wave velocity and Poisson ratio are respectively β = 1000 m/s and ν=1/3 inside the valley, and β= 2500 m/s and ν=1/4 in the halfspace.

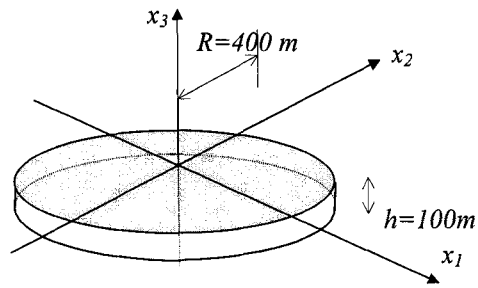

Figure 8. 3-D cylindrical inclusion subjected to the vertical incidence of plane waves.

The seismic response of this geological configuration to the vertical incidence of shear waves, directed along x_2, has been studied elsewhere (Faccioli et al., 1997; Paolucci, 1999a), using a very accurate pseudo-spectral method. Elaborating the results, the first two mode-shapes have been obtained. The fundamental shear mode and the first higher mode are depicted on the right-hand side of Figure 9, that shows the horizontal displacement along x_2, in the plane x_3=0. They occur at 2.65 Hz and 3.1 Hz, respectively. For reference, the first 1-D shear resonance frequency is $\beta/4h$=2.5 Hz.

Based on the previous numerical results and disregarding the x_1 and x_3 components of motion, the following set of mode-shapes is chosen for the problem at hand:

$$f(x_1,x_2,x_3) = 1 - \frac{{x_1}^2}{a^2} - \frac{{x_2}^2}{b^2} \tag{21}$$

$$\hat{\psi}_1(x_1,x_3) = 0 \tag{22a}$$

$$\hat{\psi}_2(x_1,x_3) = \cos^r\left[\frac{\pi}{2}\left(1 - f(x_1,x_2,x_3)\right)\right]\sin^{(2s+1)}\left[\frac{(n+1)\pi}{2}\left(1+\frac{{x_1}^2}{a^2}\right)\right]\cos^t\left(\frac{(2m+1)\pi}{2}\frac{x_3}{h}\right) \tag{22b}$$

$$\hat{\psi}_3(x_1,x_3) = 0 \tag{22c}$$

where, in the case under study, $a = b = R$. As for the 2-D case, this set of mode-shapes satisfies only the geometric boundary conditions.

The proposed approach has been followed to estimate the two first resonance frequencies of the cylindrical inclusion. Introducing Equation 22 in the right-hand side of Equation 7 and finding the minimum as a function of the parameters r, s, t (with m=0), the

first (n=0) and the second (n=1) shear resonance frequencies have been obtained. The corresponding mode-shapes (r=1, s=0, t=1) are illustrated in Figure 9 (left-hand side). Although the mode-shapes differ from the numerical ones, the first resonance frequency approximated by the present method is 2.8 Hz, i.e., 5% larger than the numerical one, while a perfect agreement is obtained for the second shear resonance frequency.

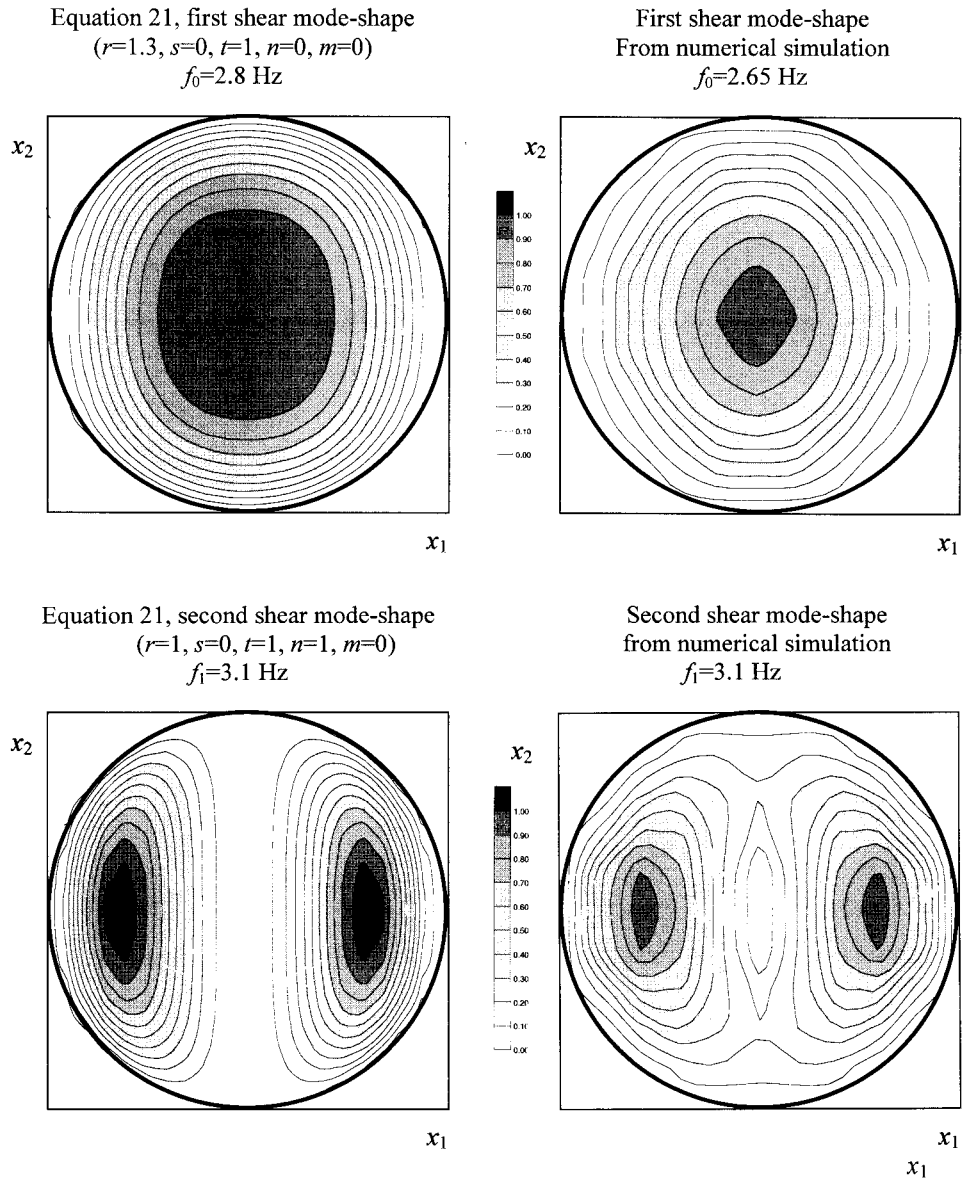

Figure 9. Right: Horizontal (x_2) component of displacement at the surface of the 3-D cylindrical inclusion calculated at the two first resonance peaks. Results from a numerical simulation using a pseudo-spectral approach. Peak values are normalized to unity. Left: Gray-scale plot of Equation 22, for the approximation of the first (n=0, upper plot) and second (n=1, lower plot) mode-shapes of the 3-D inclusion. The other parameters of (22) are set to r=1, s=0, t=1, m=0.

The mode-shapes (Equation 22) can be extended to other simple valley shapes such as the elliptical and cosine 3-D valleys, described by the following functions:

$$f(x_1,x_2,x_3)=1-\frac{x_1^2}{a^2}-\frac{x_2^2}{b^2}-\frac{x_3^2}{h^2} \qquad \text{(elliptical 3-D valley)} \qquad (23a)$$

$$f(x_1,x_2,x_3)=\cos\left(\frac{\pi}{2}\sqrt{\frac{x_1^2}{a^2}+\frac{x_2^2}{b^2}}\right)-\frac{x_3}{h} \qquad \text{(cosine 3-D valley)} \qquad (23b)$$

For the case of a cosine 3-D valley, setting $a = b$, an extensive parametric study was performed by Jiang and Kuribayashi (1988), using a boundary element approach. The approximated resonance frequencies obtained by the present simplified procedure are compared with those of the quoted paper in Figure 10, as a function of the shape ratio h/a (continuous lines). An excellent agreement is found for shape ratios larger than about 0.4, i.e., when 3-D effects are more pronounced. The agreement gets worse for smaller shape ratios, with errors up to ~20%, showing that the proposed mode-shapes are no longer suitable when the geometry approaches a 1-D configuration. The shear resonance frequencies for the second mode (n=1) are also shown in Figure 10. As in the 2-D case, the second mode shear resonance frequencies exceed the first mode ones by 70% approximately.

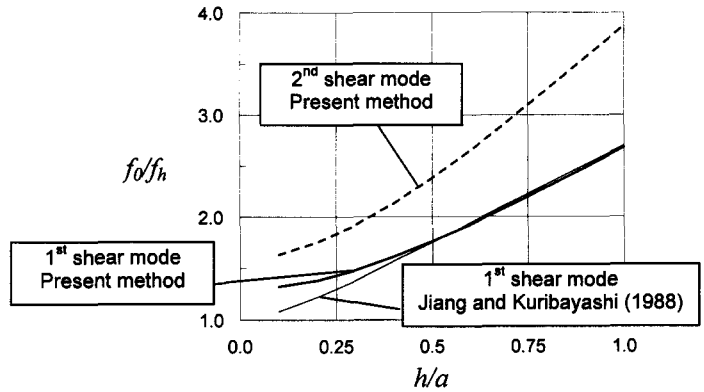

Figure 10. Comparison of the fundamental resonance frequencies of 3-D cosine-shaped axi-symmetric alluvial valleys calculated according to the empirical formula of Jiang and Kuribayashi (1988), with the results of the present method. The frequencies of the second mode calculated by the present method are also shown.

APPLICATION TO SV MODES IN NON-HOMOGENEOUS ASSYMETRIC VALLEYS

In this section, the proposed approach is applied to SV modes in realistic geological configuration, such as non-homogeneous asymmetric 2-D alluvial valleys. Let the bedrock-valley interface be defined by the following equation:

$$f(x_1,x_3)=\left(1+\frac{x_1}{a}\right)\left(1-\frac{x_1}{a}\right)^{\frac{1-\zeta}{1+\zeta}}-(1+\zeta)(1-\zeta)^{\frac{1-\zeta}{1+\zeta}}\frac{x_3}{h}. \qquad (24)$$

As shown in Figure 11, Equation 24 defines a set of asymmetric valley shapes with half-width a, depth h, and deepest position at $x/a=\zeta$. Realistic shapes may be obtained in the range $-0.5 \le \zeta \le 0.5$. In the case under study, the parameters a=200m, h=80m and ζ=-0.4 have been considered, together with the soil profile indicated in Figure 12. To check the accuracy of the proposed method, the seismic response of the valley has been first analysed using an innovative and highly efficient numerical code for seismic wave propagation in 2-D/3-D soil configurations (Casadei and Gabellini, 1997 and 1998), based on a hybrid finite-element / spectral-element solver (Lahaye et al., 1997).

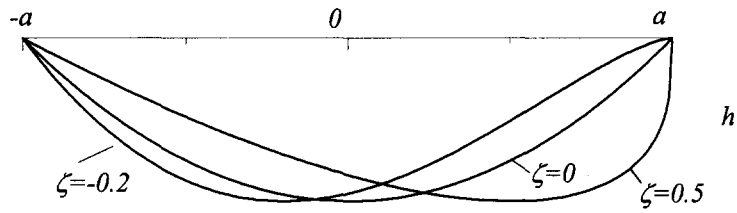

Figure 11. Different shapes of the bedrock-valley interface, as a function of parameter ζ in Equation 24.

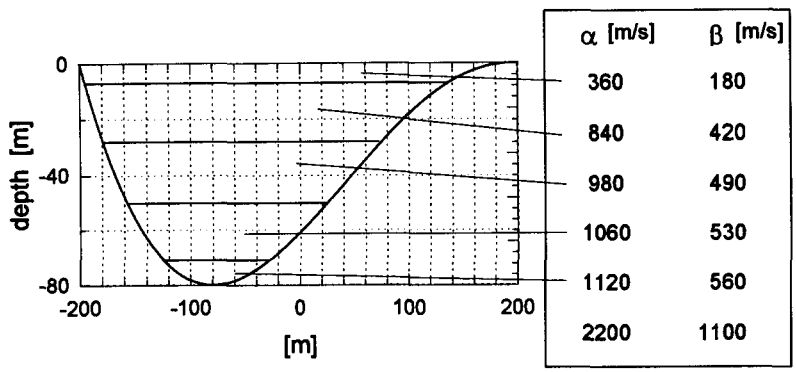

Figure 12. Non-homogeneous asymmetric alluvial valley.

The valley has been subjected to the vertical incidence of SV plane waves, with Ricker-type time dependence and frequency peak at 2 Hz. Spectral amplification functions have been calculated through spectral ratios of the response at various surface receivers with respect to the input signal. Such functions, illustrated in Figure 13, show a first peak at 2.2 Hz, affecting all surface receivers, that is to be attributed to the first shear (SV) resonance frequency of the whole valley. Higher 2-D resonance frequencies are not visible, since they are overshadowed by the 1-D shear-resonance frequencies due to the shallowest layers. The results of the present approach are also shown in Figure 13, and are obtained using a mode-shape defined by Equation 19, with the bedrock/valley interface $f(x_1,x_3)$ described by Equation 24. The estimated first resonance frequency is 2.58 Hz, that exceeds the numerical one by 17% approximately. The higher resonance frequency estimated by this method is 3.14 Hz, but it cannot be compared with the numerical simulations for the reasons mentioned previously.

The error obtained by the present method is larger then that calculated in the previous homogeneous cases. As a matter of fact, the strong vertical irregularities of the soil profile prevent a simple approximation of the displacement field, so that resonance frequencies

substantially larger than the true ones are expected. However, the error is reasonable, especially if the large uncertainties involved in the determination of the actual soil profile are taken into account. Note that the numerical code available to the writer allows only P-SV wave propagation analyses in 2-D. However, as indicated by the previous examples on homogeneous valleys, the errors for the SH case should be qualitatively similar to those obtained for the SV one.

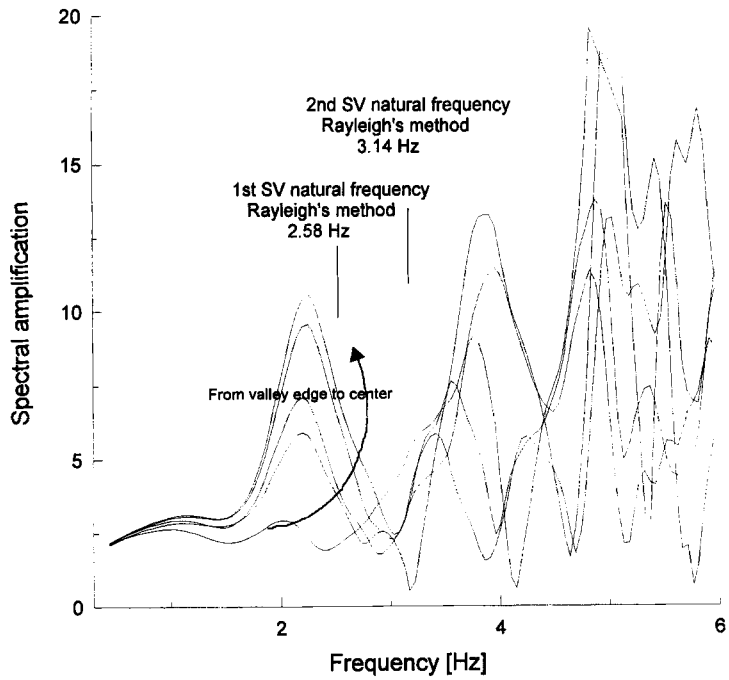

Figure 13. Spectral amplification functions calculated with the hybrid numerical code at different location at the surface of the valley of Figure 12, for incident SV waves. The resonance frequencies corresponding to the first two mode-shapes, calculated by the present method, are indicated.

Subsequently, a real geological configuration has been considered, in order to show a practical application of the method. It consists of the Adige River Valley, a sediment filled deep alluvial valley in Northern Italy. The 2-D seismic response of Adige Valley has been studied by Faccioli and Vanini (1998), with reference to the cross-section corresponding to the northern side of the town of Trento. The cross-section is illustrated in Figure 14 (continuous line), together with the dynamic properties of the soil layers. The numerical tool used for the analysis is the same hybrid solver mentioned before. The shape ratio of the valley (depth over half-width) approaches unity, so that 2-D effects in the seismic response are expected to be rather pronounced. Besides, strong irregularities in the soil profile are present, especially in the shallowest layers. These soil conditions make it quite difficult to rely on the common estimates of the fundamental frequencies of vibration at surface sites, typically based upon a 1-D approximation.

A set of spectral amplification functions of the horizontal components of motion at various surface receivers calculated by the hybrid numerical code is shown in Figure 15. These functions show two resonance frequencies at f_0 = 0.58 Hz and f_1 = 0.95 Hz approximately, that appear at every surface site of the valley, with different amplification

levels, thus denoting 2-D resonance modes. For higher frequencies, the 1-D resonance linked to the shallowest layers tends to dominate site response, so that higher 2-D resonance modes are not visible.

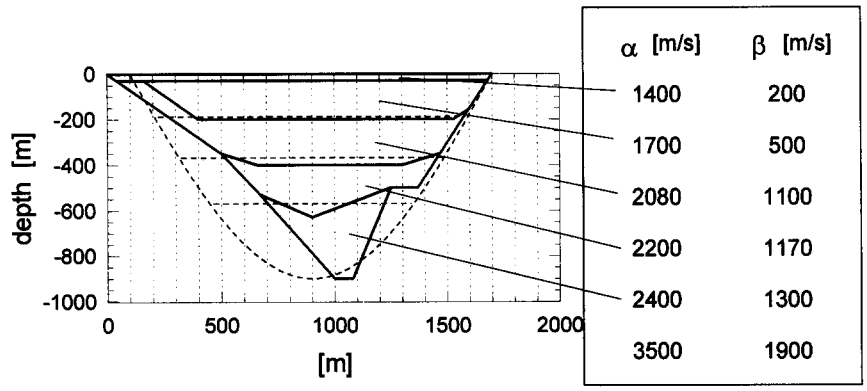

Figure 14. Cross-section of Adige Valley considered for numerical simulation with a hybrid spectral element – finite element code (continuous line). Cosine-shaped valley used for application of the present method (dashed line).

Using the present method, the valley has been approximated by a cosine shape (Equation 16b), as shown in Figure 14. The mode-shape (Equation 19) has been introduced in Equation 7, and the appropriate values of the elastic constants have been used at different depths, to take into account the variability with depth of the dynamic properties of soil. The shear resonance frequencies obtained are indicated in the upper side of Figure 15. The error of the present method is about 18%, similar to that obtained previously.

From the previous examples it is important to note that in most practical cases the resonance frequencies of 2-D alluvial valleys may be detected only in the low-frequency range, where the 1-D amplification effects due to the shallowest layers is not prominent. In the case of a deep valley, such as Adige Valley with shape ratio h/a=1.1, it has been possible to detect the first two natural frequencies due to 2-D resonance, while in the case of an asymmetric valley with h/a=0.4, only the first one is visible. Therefore, estimating 2-D resonance frequencies higher than the first two ones seems to be useless for most practical applications.

CONCLUSIONS

A simple procedure based on Rayleigh's method has been developed and tested for estimating the shear resonance frequencies of alluvial valleys. It essentially consists of the following steps:

- select a set of admissible shapes for the desired natural mode;
- calculate the maximum strain and kinetic energies corresponding to the desired mode and selected mode-shape, through simple surface or volume integration subroutines that can be found in any numerical library;
- find the shape that minimizes the ratio at the right-hand side of inequality (Equation 7).

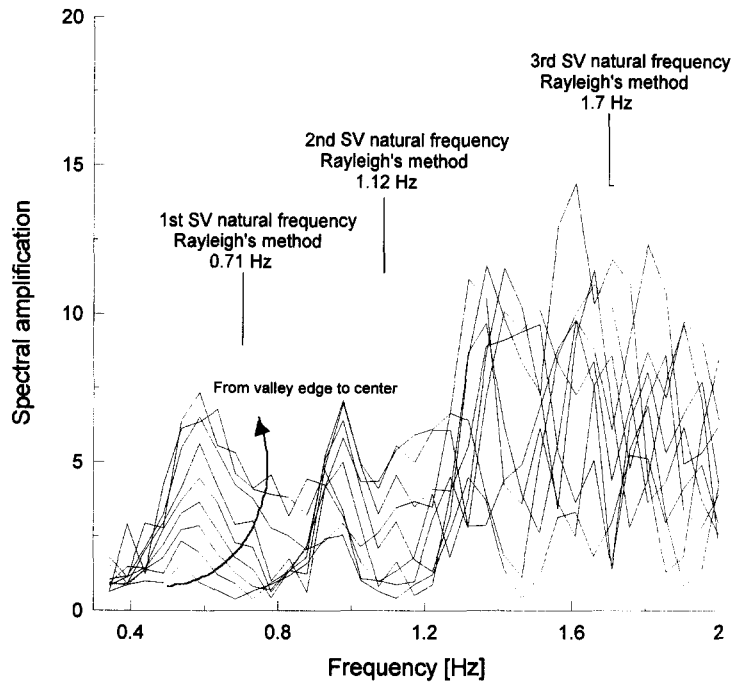

Figure 15. Spectral amplification functions calculated with the hybrid numerical code at different location at Adige Valley surface, for incident SV waves. The resonance frequencies corresponding to the first three natural modes, calculated by the present method, are indicated.

Using simple-shaped homogeneous valleys, both in 2-D and 3-D, it has been shown that satisfactory results are obtained even if the selected mode-shape does not match the stress-free boundary condition at the surface. Indeed, as demonstrated by Meirovitch (1967), the natural conditions on stresses at boundaries can be relaxed, and the approximated mode-shapes can be chosen in the larger class of admissible functions that satisfy only the geometric boundary conditions.

The approximated mode-shapes (Equations 19 and 22) are proposed, for 2-D and 3-D geometries respectively, that have been found to approach closely the results of sophisticated and time-consuming numerical simulations, especially for shape ratios h/a (valley depth over half-width) larger than about 0.3. This is the range where the 1-D theory is no more suitable and 2-D/3-D site effects appear more clearly.

The procedure, introduced for homogeneous media, can be easily extended to complex problems involving heterogeneous materials, as it has been demonstrated in the case of an asymmetric non-homogeneous valley and of a real deep sedimentary basin (Adige Valley, Italy). The prediction errors are negligible for homogeneous alluvial valleys, and grow up to about 20% for the non-homogeneous case. Besides, it is worth noting that the predicted values generally provide an upper bound of the actual ones.

The present work has been limited to the evaluation of shear resonance frequencies, that represents the most interesting case for practical applications. A similar approach can also be used for the estimation of bulk resonance frequencies. The application of the proposed approach to the evaluation of shear resonance frequencies of topographic irregularities is shown by Paolucci (1999b).

The main limitation of the proposed procedure is that no information can be extracted about the actual amplification values at resonance. However, such values are seldom correctly predicted even by the most sophisticated methods, since they strongly depend on small-scale local heterogeneities of the soil profile, as well as on material dissipation. Note that the assumption of linear behavior of soil materials, that is implicit in Rayleigh's approach, can be relaxed if an appropriate equivalent linear soil profile is introduced, that takes into account the elastic moduli reduction with the deformation level.

The proposed method may prove helpful for filling the gap between research studies on complex 2-D/3-D seismic site effects and their practical application, as for several typical problems as:

- Interpretation of field data from weak or strong motion arrays, that is generally carried out either by means of the 1-D theory or by complex numerical simulations.
- Determination of the frequency band where peak amplification is likely to occur. Even for complex geological configurations, the user can easily assess in which frequency band 1-D resonance will differ significantly from the 2-D or 3-D one, and decide whether performing more sophisticated analyses of site effects. This is important in assessing the applicability of standard code spectral shapes at sites on complex 2-D/3-D configurations.
- Parametric analyses as a function of soil properties.

The proposed method can be easily implemented using standard subroutines for integration in 2-D/3-D domains, such as those provided by Press et al. (1992), and choosing the mode-shapes suggested in this paper.

The interested reader may download the numerical code for 2-D non-homogeneous valleys at the author's web site (*http://www.stru.polimi.it/sismica/paolucci/roberto.html*).

ACKNOWLEDGEMENTS

The author is indebted to Ezio Faccioli and to Francisco J. Sánchez-Sesma for the careful reading of the manuscript and the useful suggestions. The comments of an anonymous reviewer helped improving the paper. The numerical simulations with the hybrid numerical code were performed by Manuela Vanini and Pietro Colli, of the Politecnico di Milano. The cooperation of the Geological Survey of the Trento provincial administration in providing data is gratefully acknowledged. This work has been partly funded under the EC grant FMRX-CT96-0022, within the Training and Mobility of Researchers program.

REFERENCES

Aki, K., 1993, Local site effects on weak and strong ground motion, *Tectonophysics*, **218**, 93–111.

Bard P.-Y. and Bouchon, M., 1985, The two-dimensional resonance of sediment filled valleys, *Bull. Seism. Soc. Am.*, **75**, 519–541.

Casadei, F. and Gabellini, E., 1997, Implementation of a 3-D coupled spectral element/finite element solver for wave propagation and soil-structure interaction simulations, Part I – Models, *Tech. Rep. of the Joint Research Centre for the EC Environment and Climate Project TRISEE (3-D Site Effects and Soil-Foundation*

Interaction in Earthquake and Vibration Risk Evaluation), EC EUR 17730 EN, Ispra, Italy.

Casadei, F. and Gabellini, E., 1998, Implementation of a 3-D coupled spectral element/finite element solver for wave propagation and soil-structure interaction simulations, Part II – Numerical examples, *Tech. Rep. of the Joint Research Centre for the EC Environment and Climate Project TRISEE (3-D Site Effects and Soil-Foundation Interaction in Earthquake and Vibration Risk Evaluation)*, EC EUR 18051 EN, Ispra, Italy.

Chávez-García, F. J. and Faccioli, E., 1999, Complex site effects and building codes, *Journal of Seismology*, in press.

Chen, W. F and Liu, X. L., 1990, Limit analysis in soil mechanics, *Developments in Geotechnical Engineering*, Vol. 52, Elsevier, New York.

Clough, R. W. and Penzien, J., 1975, *Dynamics of Structures*, McGraw-Hill, Inc.

Dobry, R., Oweis, I., and Urzua, A., 1976, Simplified procedures for estimating the fundamental period of a soil profile, *Bull. Seism. Soc. Am.*, **66**, 1293–1321.

Faccioli, E., Maggio, F., Paolucci, R., and Quarteroni, A., 1997, 2-D and 3-D elastic wave propagation by a pseudo-spectral domain decomposition method, *Journal of Seismology*, **1**, 237–251.

Faccioli, E. and Vanini, M., 1998, Studio della risposta sismica locale nella zona di Trento Nord, *Tech. Rep. for the Autonomous Province of Trento*, Italy (in Italian).

Frankel, A. and Vidale, J., 1992, A three-dimensional simulation of seismic waves in the Santa Clara Valley, California, from a Loma Prieta aftershock, *Bull. Seism. Soc. Am.*, **82**, 2045–2074.

Graves, R., 1998, Three-dimensional finite-difference modeling of the San Andreas Fault: source, parameterization and ground-motion levels, *Bull. Seism. Soc. Am.*, **88**, no. 4.

Jiang, T., and Kuribayashi, E., 1988, The three-dimensional resonance of axi-symmetric sediment-filled valleys, *Soils and Foundations*, **28**, 130–146.

Lahaye, D.J.P., Maggio, F., and Quarteroni, A., 1997, Hybrid finite — spectral element approximation of wave propagation problems, *East-West J. Num. Math.*, **5**, 211–231.

Meirovitch, L., 1967, *Analytical methods in vibrations*, The Macmillan Co., Collier-Macmillan Ltd., London.

Olsen, K., Archuleta, R. and Matarese, J., 1995, Three-dimensional simulation of a magnitude 7.75 earthquake on the San Andreas fault, *Science*, **270**, 1628–1632.

Paolucci, R., Suárez, M. and Sánchez-Sesma, F. J., 1992, Fast computation of SH seismic response for a class of alluvial valleys, *Bull. Seism. Soc. Am.*, **82**, 2075–2086.

Paolucci, R. and Pecker, A., 1997, Seismic bearing capacity of shallow strip foundations on dry soils, *Soils and foundations*, **37**, 95–105.

Paolucci, R., , E., and Maggio, F., 1999, 3-D response analysis of an instrumented hill at Matsuzaki, Japan, by a spectral method, *Journal of Seismology*, in press.

Paolucci, R., 1999a, Numerical evaluation of the effect of cross-coupling of different components of ground motion in site response analyses, *Bull. Seism. Soc. Am.*, accepted for publication.

Paolucci, R., 1999b, Fundamental vibration frequencies of 2-D geological structures, Proc. 2nd Int. Conf. on Earthquake Geotechnical Engineering, Lisboa, Portugal, June 21–25 1999.

Prentis, J. M., 1970, *Dynamics of mechanical systems*, Longman. 540 pp.

Press, W. H., Teukolsky, S. A., and Vetterling, W. T., 1992, *Numerical recipes in Fortran – The art of scientific computing*, Cambridge University Press, 963 pp.

Rodríguez-Zúñiga, J. L. Sánchez-Sesma, F. J., and Pérez-Rocha, L. E., 1995, Seismic response of shallow alluvial valleys: the use of simplified models, *Bull. Seism. Soc. Am.*, **85**, 890–899.

Schnabel, P. B., Lysmer, J., and Seed, H. B., 1972, SHAKE. A computer program for earthquake response analysis of horizontally layered sites, *Tech. Rep. n. 72-12*, Earthquake Engineering Research Center, Berkeley, CA.

Schreyer, H., 1977, One-dimensional elastic waves in inhomogeneous media, *ASCE J. Engineering Mechanics Div.*, 979–991.

Uniform Building Code, 1997, Volume 2 – *Structural Engineering Design Provisions. Division IV – Earthquake Design*, International Conference of Building Officials.